CRYSTAL GROWTH & DESIGN

Article

pubs.acs.org/crystal

Application of Continuous Crystallization in an Integrated Continuous Pharmaceutical Pilot Plant

Haitao Zhang, Richard Lakerveld, Patrick L. Heider, Mengying Tao, Min Su, Christopher J. Testa, Alyssa N. D'Antonio, Paul I. Barton, Richard D. Braatz, Bernhardt L. Trout, Allan S. Myerson, Klavs F. Jensen, and James M. B. Evans*

Department of Chemical Engineering, Massachusetts Institute of Technology, 77 Massachusetts Avenue, Cambridge, Massachusetts 02139, United States

ABSTRACT: Real-time control using process analytical technology (PAT) tools is required for the implementation of continuous crystallization within integrated continuous manufacturing (ICM) of pharmaceuticals. However, appropriate selection of PAT tools is challenging, and the design and operation of automated control loops for continuous crystallization within a continuous pharmaceutical process brings forward important questions. This paper discusses the process design and operation of a continuous reactive crystallization of aliskiren hemifumarate as part of an ICM pilot plant. Several PAT tools were used within automated control loops to satisfy specifications on the critical materials attributes of the crystallization process. The operational performance of the process was maintained for periods of time over 100 h. The purity of the targeted product exceeded 99%, and the process yield reached 91.4%.

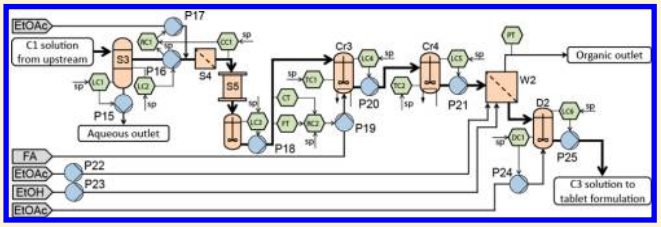

INTRODUCTION

The concept of continuous manufacturing to address key challenges faced by the pharmaceutical industry has gained significant interest.[1−4] A number of research programs related to this topic have been sponsored by pharmaceutical companies, including Pfizer, Novartis, Merck, and Eli Lilly. The Novartis-MIT Center for Continuous Manufacturing has developed a seamless, end-to-end pilot plant for continuous manufacturing of pharmaceuticals including new pieces of technologies to support integrated continuous manufacturing (ICM).[5] Continuous crystallization plays a critical role within ICM processes.[1,2] Previous studies have investigated different styles of continuous crystallizers including mixed-suspension mixed-product removal (MSMPR),[6−9] plug-flow (PF),[10] and continuous oscillatory baffled crystallizers.[11] Furthermore, process modeling has been employed for process design and optimization.[12−16] However, previous research efforts mainly focused on the process development and the technological innovation of the continuous crystallization unit. There is little research reported on the integration of continuous crystallization into an entire continuous pharmaceutical manufacturing process.[17]

Significant progress on the control of crystalline product quality has been achieved with a focus on different aspects of the crystallization process including the particle size distribution, polymorphism, purity, and solvent.[18−26] Previous research has centered on studying different control strategies and process analytical technology (PAT) tools with a strong emphasis on batch crystallization processes. The aim of this contribution is to investigate the performance of a continuous crystallization step operated for a prolonged period of time within an ICM process. The integration of different unit operations and the steady-state operation of those unit operations are of primary concern. The aim is to keep the critical material attributes (CMAs) for each unit operation including the continuous crystallization units within an accepted range at all times through the control of critical process parameters (CPPs). Consequently, the control strategy should possess the capability to tolerate variations from upstream units and should minimize disturbances that propagate to downstream units. Therefore, the selection and implementation of PAT tools and the design of a control strategy are of vital importance for successful ICM of pharmaceuticals. Such a control strategy would rely on automated feedforward and feedback control loops.

Previously, we presented the application of a multistage cascade MSMPR continuous crystallization system at 50 mL scale operated independently of a pharmaceutical manufacturing process and demonstrated experimentally its capability to crystallize different organic compounds.[7,8] In this work, this process was scaled up to 15 L and integrated with online control to mitigate disturbances from the process. Aliskiren hemifumarate was the target drug substance. The ICM pilot plant has a throughput of 45 g of active pharmaceutical ingredient (API) per hour (360 tablets/h). The process started with advanced chemical intermediates and produced tablets. The process included two key chemical reactions, two liquid−liquid extraction steps, a reactive crystallization to form the final

Received: October 22, 2013
Revised: March 5, 2014
Published: March 20, 2014

   dx.doi.org/10.1021/cg401571h | *Cryst. Growth Des.* 2014, 14, 2148−2157

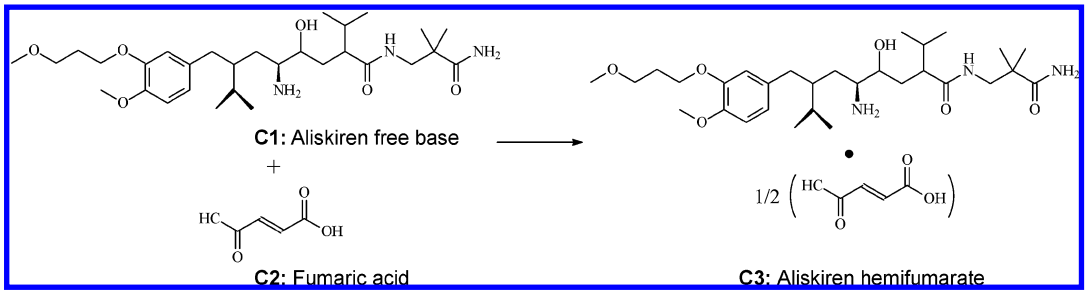

Figure 1. Formation reaction of aliskiren hemifumarate.

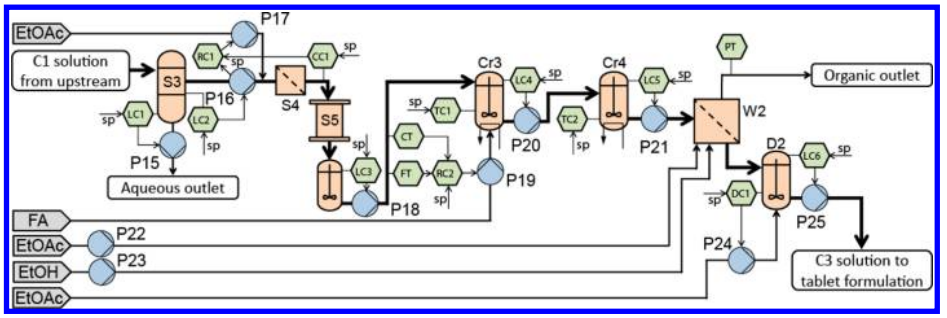

Figure 2. Schematic of the portion of the ICM process to produce tablets containing aliskiren hemifumarate around the continuous crystallization of the API. Automated control loops and PAT devices are indicated by green hexagons (S3, S4, S5, Cr3, Cr4, W2, D2). P - pump; TC - temperature controller; CT - concentration transmitter; FT - flow transmitter; RC - ratio controller; S - separation; Cr - crystallization vessel; LC - level controller; PT - pressure transmitter; W - filter/wash; D - dilution tank; DC - density controller; CC - concentration controller; FC - flow controller; E - extruder; MD - mold; sp - control set point.

API salt, an additional crystallization step, two filtrations, drying, extrusion, and molding—all in a fully continuous fashion. Typical PAT tools that were used throughout the process include level sensors, flow meters, density meters, ultraviolet (UV) flow cells, infrared (IR) flow cells, and pH meters. Typical actuators that were present to manipulate the performance of the process included pumps, heaters, and coolers. The PAT tools and actuators were all connected to an integrated control system (Siemens, PCS7) where they were used to implement a plant-wide control strategy based on automated control loops.[27]

The work presented in this paper is part of a larger collection of work related to a continuous pharmaceutical pilot plant that has been constructed within the Novartis-MIT Center for Continuous Manufacturing. Our experimental findings related to different aspects of the pilot plant have resulted in papers submitted to different journals. The papers include a detailed discussion of the design and performance of the entire ICM system focusing on the final product has been reported,[5] a report about the chemical synthesis steps within the pilot plant,[28] a discussion of the control system for the complete pilot plant, and the current paper about the application of continuous crystallization in the pilot plant.

Herein, we report the results and conclusions from our study on the integration of continuous crystallization of aliskiren hemifumarate within an ICM pilot plant. The work demonstrates how to integrate the continuous crystallization step into the entire plant and how to achieve steady-state operation through suitable selection of PAT tools and automated control loops. The paper is structured as follows. First, the materials involved in the crystallization step and the selected PAT and automated control loops are outlined. Second, results are described in terms of (1) automated conditioning of the feed material received from upstream units via a combined automated feedback and feedforward control scheme, (2) automated dosage of the reagents by feedforward control, (3) level control of the continuous crystallizers via feedback control, and (4) automated workup of the produced slurry by the feedback control loops. This is followed by characterization of the crystallized API in terms of X-ray powder diffraction (XPRD) patterns, crystal morphology, and particle size.

EXPERIMENTAL SECTION

Materials. Aliskiren free base (C1) arrived from upstream units as a clear solution in ethyl acetate with a number of dissolved impurities in small quantities. Fumaric acid (C2) was purchased from Sigma Aldrich and used without any further purification. Ethyl acetate (EtOAc) (ACS reagent, ≥99.5%) and ethanol (EtOH) (ACS reagent, ≥99.5% (200 proof), absolute) were also purchased from Sigma Aldrich.

Process Description. The continuous manufacturing process has been described generally elsewhere.[5] Here we provide a detailed description of the continuous crystallization units used to synthesize and crystallize the target API and the related upstream and downstream unit operations (Figure 2).

The aliskiren free base (C1) is generated in an upstream reactor,[28] and the two-phase reaction product stream is sent into a 2-L settling tank S3 where the aqueous phase is disposed and the organic phase (≈30 wt % C1 solution in ethyl acetate) is sent into the reactive-crystallization section of the plant as one of the feed materials. The settling tank S3 is equipped with two ultrasonic level sensors (Omega LVCN414 level sensor, Omega Engineering, Inc.) to maintain the level of both phases close to the desired set point through the level control loops LC1 and LC2. Subsequently, the organic stream with C1 is diluted with a stream of ethyl acetate via a ratio controller RC1 based on the organic phase flow rate. The flow rate of the C1 solution fluctuates as a result of active level control in the settling tank. The C1 solution is diluted before entering the reactive cooling crystallization for two reasons. First, experimental results showed that C1 nucleation was difficult to achieve at higher concentrations (>7 wt %) due to C1

dx.doi.org/10.1021/cg401571h | Cryst. Growth Des. 2014, 14, 2148−2157

leaving the solution as an oil. Second, slurries formed from reactive cooling crystallization at higher C1 concentrations (>7 wt %) are too thick to reliably pump.

The C1 solution sometimes entrains some aqueous phase with NaCl that precipitates when diluted by ethyl acetate. The stream is therefore passed through a number of microfiltration membranes (0.45 μm Pellicon XL 50, Millipore) to remove any solid NaCl that may have precipitated after dilution. The reactive crystallization step requires an anhydrous environment and a constant composition of the C1 stream, so the diluted stream passes through a UV flow cell (HR2000+, Ocean Optics) that monitors the absorption at 300 nm to enable control of the C1 concentration going downstream. The control loop is a combined feedforward and feedback cascade control loop in which an outer loop manipulates the set point of an inner loop (ratio controller). The aim of the combined feedforward and feedback control is to isolate fast disturbances (originating from the level control upstream) from slow disturbances (i.e., drifts in concentration of C1 in the settling tank). The UV flow cell measurement is converted to concentration based on a calibration model. A 94% pure C1 solution in ethyl acetate consistent with the real process material is used to calibrate the UV sensor resulting in a linear calibration curve. The organic stream then passes through two 35-L columns packed with 3 Å molecular sieves to remove any residual water. The column is sized based on the capacity required to operate the process for at least 2 weeks. The stream exits the column into a break tank, which acts as a buffer vessel before the crystallizers. An automated feedback level-control loop LC3 (with Omega LVCN414 level sensor) determines the flow rate of C1 solution going into the continuous crystallization process. The dosage of C2 into the crystallizers is crucial to obtain the desired product identity and to ensure that sufficient solid mass remains in the crystallizer. To achieve precise dosage of C2, the flow of C1 solution passes through another UV flow cell (HR2000+, Ocean Optics) where the concentration of C1 is measured and used in an automated feedforward control loop RC2 to manipulate the flow rate of C2 solution into Crystallizer 3. C2 is dissolved in a mixture of ethanol and ethyl acetate (1:1 solvents mixture, 5 wt % C2 solution) according to

$$Q_{C2} = \frac{Q_{C1}\rho_{C1,s}C_{C1}M_{w,C2}}{2\rho_{C2,s}C_{C2}M_{w,C1}} \quad (1)$$

where Q_{C1}: flow rate of C1, Aliskiren free base solution (m^3/s); Q_{C2}: flow rate of C2, fumaric acid solution (m^3/s); $\rho_{C1,s}$: density of C1 solid, Aliskiren free base (kg/m^3); $\rho_{C2,s}$: density of C2 solid, fumaric acid (kg/m^3); C_{C1}: concentration of C1 in the feeding solution (kg/kg); C_{C2}: concentration of C2 in the feeding solution (kg/kg); $M_{w,C1}$: molecular weight of C1 (kg/mol); $M_{w,C2}$: molecular weight of C2 (kg/mol).

Crystallizer 3 is a 15-L jacketed glass vessel with an overhead stirrer (Heidolph electronic high-torque overhead stirrer). An anchor agitator with square cross middle blade is employed and is typically operated at 120 rpm.

The C1 and C2 solution are fed in a molar ratio of 1.0:0.55 of C1/C2. The temperature in Crystallizer 3 is controlled at 20 °C by a thermostatic bath (Thermo NESLAB, RTE-7 Digital Plus) with an external Pt-100 resistance thermometer. The salt formation reaction and the crystallization of the final drug substance occur simultaneously in Crystallizer 3. The slurry is transferred into Crystallizer 4 with a peristaltic pump (Masterflex L/S). Crystallizer 4 is also a 15-L jacketed glass vessel with an overhead stirrer (Heidolph electronic high-torque overhead stirrer) typically operating at 120 rpm. The flow rate is controlled by an automated feedback level-control loop LC4 to maintain a level corresponding to a nominal residence time of 4 h which was set based on the crystallization kinetics.[8] The level is monitored by an ultrasonic level sensor (Omega LVCN414). The temperature of Crystallizer 4 is controlled at −10 °C by a thermostatic bath (Lauda, Proline RP 845) with an external Pt-100 resistance thermometer. At the end of the crystallization step, the slurry of the final drug substance, C3, is pumped into a continuous filter (wash-filtration 2) where the crystals are filtered and washed with ethyl acetate. The flow rate of the slurry is controlled by an automated feedback level-control loop LC5 similar to the one for Crystallizer 3.

The impeller Reynolds number, Re, the impeller Power number, N_p, the just suspended stirring speed, N_{js}, and the power consumption per unit volume, P/V were calculated to estimate the mixing performance in the crystallizers at steady state operation (see Table 1). The values

Table 1. Mixing Properties in the Two Crystallizers during Steady-State Operation

Parameters	Crystallizer 3	Crystallizer 4
impeller Reynolds number, Re[29a]	1.3×10^5	8.5×10^4
impeller power number, N_p[29]	0.35	0.35
$N_p^{1/3}$Re[a]	8.9×10^4	6.0×10^4
just-suspended stirring speed, N_{js} [rpm][30,31]	43	46
torque [N·m]	1.9	3.8
normalized power consumption, P/V [W/m^3]	4.5×10^2	8.8×10^2

[a]The criteria for turbulent regime is Re > 10000, or $N_p^{1/3}$Re > 6370.

of Re are larger than 10 000 in both of the crystallizers, which indicates that the operations were in turbulent regime with the applied impeller geometry and rotational speed (120 rpm).[29] Furthermore, the so-called just-suspended stirring speed was estimated as 43 and 46 rpm in Crystallizers 3 and 4, respectively,[30,31] which indicates that the operational impeller speed of 120 rpm was high enough to suspend the crystals. The power consumption per unit volume, which is a measure of mixing intensity, was calculated based on the torque data acquired during the experiments.

Finally, the wet cake exiting the filter is collected in a 5-L glass vessel with an overhead stirrer (Heidolph electronic high-torque overhead stirrer) typically operated at 120 rpm. A stream is pumped out of the tank and passed through a density flow cell (Anton Paar DPRn 417) before being returned to the vessel. The density measurement is used to calculate the solid loading in the vessel. The solid loading is controlled by an automated feedback control loop DC1 that manipulates the flow rate of an ethyl acetate feed stream. The solid loading is an important CMA for the performance of the dryer downstream. A peristaltic pump delivers the slurry into a continuous dryer. All data produced are archived every 10 s by an integrated control system (Siemens, PCS7). To summarize the control structure and the operation of the plant, an overview of the measured, manipulated, and controlled variables and the nominal set points of all control loops illustrated in Figure 2 is given in Table 2.

In general, when deciding on the control loop pairing for an integrated unit operation, the impact on the plant as a whole has to be taken into account. Model-based simulations of a process that was inspired by the pilot plant have demonstrated that the C3 concentration of the slurry in the dilution tank has a significant effect on the final product quality.[27] Therefore, automated control of the yield of the crystallization step is important in addition to the discussed workup step of the produced slurry. The feedforward control loop for automated dosing of C2 aims to take corrective action before a disturbance affects the operation of the crystallizer, that is, to adjust the dosing of C2, based on a measured input disturbance (inlet concentration of C1), before the molar ratio of C1 and C2 in the crystallizer starts to deviate as a result of this input disturbance. At the end of the discussed sequence of unit operations, the concentration control loop aims to bring the critical C3 concentration in dilution tank D2 to the desired value. A large controller gain was chosen here to achieve fast responses and a small steady-state offset. Note that the selection of controlled and manipulated variables is also dictated by the availability of PAT. In this particular case, it would be desirable to augment the feedforward controller for dosing of fumaric acid with an automated feedback controller. Since feedforward and feedback control are complementary in nature (i.e., anticipation combined with correction), the combined control scheme is expected to give superior results. However, such a feedback control loop also requires the controlled variable (C1 and C2 ratio) to be measured online,

Table 2. Overview of the Measured, Controlled, and Manipulated Variables and the Nominal Set Point for Each of the Control Loops Illustrated in Figure 2

tag name	measured variable	controlled variable	manipulated variable	nominal set point
LC1	aqueous level in S3	aqueous level in S3	flow rate (P15)	1.2 L
LC2	organic level in S3	organic level in S3	flow rate (P16)	2.7 L
LC3	level in buffer tank	level in buffer tank	flow rate (P18)	0.40 L
LC4	level in Cr3	level in Cr3	flow rate (P20)	8.0 L
LC5	level in Cr4	level in Cr4	flow rate (P21)	8.0 L
LC6	level in D2	level in D2	flow rate (P25)	2.5 L
CC1	C1 concentration at inlet of S5	C1 concentration at inlet of S5	set point of RC1	7.0 wt %
RC1	flow rate (P16)	ratio of flow rates (P17/P16)	flow rate (P17)	from CC1
RC2	C1 concentration + flow rate (P18)	C1/C2 ratio	flow rate (P19)	1.0:0.55
TC1	temperature Cr3	temperature Cr3	jacket temperature	20 °C
TC2	temperature Cr4	temperature Cr4	jacket temperature	−10 °C
DC1	density of material in D2	C3 concentration in D2	flow rate (P24)	8.0 wt % (t < 148 h); 11 wt % (148 h < t < 169 h); 13 wt % (t > 169 h)

which was not possible for our studied case. This trade-off between improved process control through investments in PAT on the one hand and shortening of process development time and investments costs on the other hand is a common situation for integration of continuous crystallization in future continuous pharmaceutical plants.

Product Characterization. Compositions are measured using high performance liquid chromatography (HPLC). Mother liquor samples are taken using PTFE syringe filters with 0.2-μm pore size. An HPLC instrument (Agilent Technologies 1200 Series) with an Ascentis Express RP Amide column (2.1 × 50 mm, 2.7 μm)) maintained at 30 °C is used. The injection volume is 2.5 μL. Mobile phase A is 0.1 vol% trifluoroacetic acid in water and mobile phase B is 0.05 vol% trifluoroacetic acid in acetonitrile. The mobile phase is run in gradient mode at a constant flow rate of 0.8 mL/min. The ramp follows the schedule: initial at 15% B; 40% B at 2.37 min; 70% B at 4.04 min; 70% at 4.87 min; 15% B at 4.88 min; hold until 7.5 min and end method. Detection is performed with an Agilent 1200 Series. UV detector at 230 nm.

Chord length distributions of the solid product are measured offline with a focused beam reflectance measurement (FBRM) after the slurry sample is diluted 20 times.[32−36] The FBRM device is a Lasentec S400 probe from Mettler Toledo with a measurement range from 785 nm to 1000 μm. iXRPD patterns are recorded with a PANalytical X'Pert PRO theta/theta powder X-ray diffraction system with a Cu tube and X'Celerator high-speed detector. Crystal morphology is observed with a Zeiss Axiovert 200 optical microscope in transmission mode with a differential interference contrast polarizer and magnification range from 5× to 50×.

RESULTS AND DISCUSSION

The two-stage MSMPR continuous reactive cooling crystallization process has been operated successfully in an integrated fashion within the ICM pilot plant using automated process control. In general, the data comprise over 100 h of sustained operation with typical sampling times of 10 s for each sensor. To reveal trends clearly, the data are typically filtered by taking the median value over a period of time, which eliminates dynamics on shorter time scales that may be the result of measurement noise or short disturbances. In addition, certain time intervals are selected to demonstrate the performance of the system in more detail. This section reports the experimental findings on how to exploit PAT and process control to maintain steady-state operation including: (1) concentration control of the C1 feed solution with a UV flow cell; (2) level control of the crystallizers with level sensors; (3) C2 dosage control for the salt-formation reaction with an inline UV flow cell; and (4) C3 concentration control with an online density meter flow cell.

Concentration Control of the C1 Solution. First, we will discuss the long-term performance of the automated control loops that maintain the concentration of C1 at the entrance of the dehydration column at a desired value. Figure 3A shows the dynamic performance of the concentration of C1 over a period of 200 h. Each point in the graph is the median of measured values over a period of 100 min. The graph shows that the selected PAT tools and control loops are able to maintain long-term stability of the C1 concentration going into the dehydration column (the significant deviations from the set point at about 170 h were the result of manual cleaning of salt filters). Figure 3B presents the flow rate of the solvent feed stream that is introduced to maintain the concentration of C1 at the set point. Fluctuations occurring on different time scales can be observed. Relatively fast changes in the flow rate of solvent are the result of the behavior of the two level control loops in the settling tank situated upstream from the mixing point. Furthermore, a baseline of about 10 mL/min can be distinguished, which corresponds to the required flow rate of solvent when the level controller of the settling tank upstream is saturated; that is, the controller is programmed to provide a minimum flow rate of C1 solution to the crystallization section even when the level in the settling tank is low. This baseline trends upward slowly, which indicates that on average more solvent is required to maintain the C1 concentration at the set point toward the end of the run. Figure 3C presents the ratio of the flow rate of solvent over the flow rate of C1 solution as adjusted automatically by the outer feedback control loop. Indeed, the ratio increases throughout the run, which could be caused by a slow change in the performance of upstream units affecting the composition of the C1 solution produced. The outlier points around 100 h of operation were due to a clogging event in the upstream reaction unit.

Second, we will focus on the typical short-term performance of the C1 concentration control loops. Figure 4A shows the dynamic development of the C1 concentration before the dehydration column including two set point changes in 2.5 h. The measured concentration from the UV flow cell follows the set point changes well. The solvent flow rate added to the C1 solution is shown in Figure 4B. It can be seen that the solvent flow rate fluctuates strongly to reject the disturbances at the mixing point. For example, in the beginning of the interval, fast changes in the flow rate can be observed. In the second part of

dx.doi.org/10.1021/cg401571h | Cryst. Growth Des. 2014, 14, 2148−2157

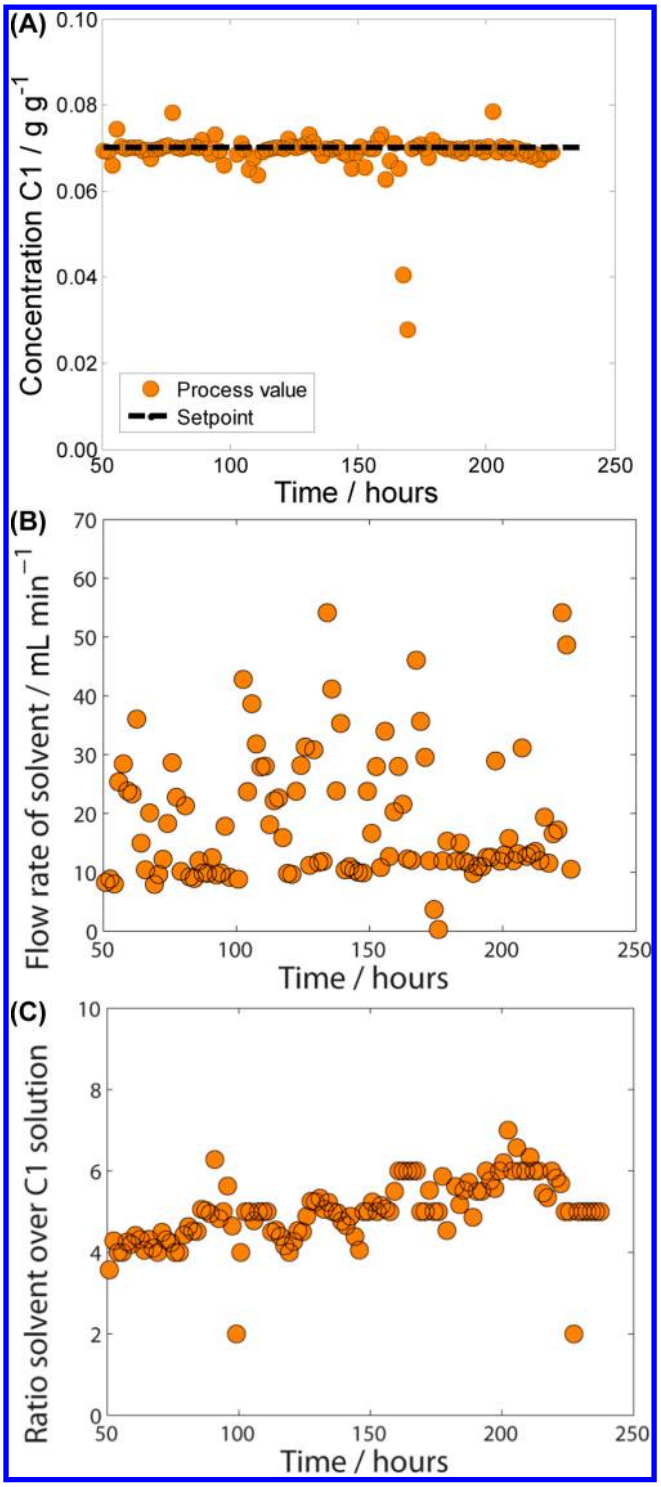

Figure 3. (A) C1 concentration (controlled variable) before entering the dehydration column during an integrated run of the end-to-end continuous pharmaceutical pilot plant. Each point represents the median value of a series of data points collected within 100 min with a sampling frequency of 0.1 Hz. The PI-control loop uses a gain of 51 g/g and an integration time of 60 s. (B) Flow rate of solvent (manipulated variable of inner ratio control loop) added to dilute the solution of C1 going into the dehydration column during an integrated run of the end-to-end continuous pharmaceutical pilot plant. Each point represents the median value of a series of data points collected within 100 min with a sampling frequency of 0.1 Hz. (C) Ratio of the flow rate of a solvent feed stream over the flow rate of C1 solution (manipulated variable of outer concentration control loop) coming from upstream units during an integrated run of the end-to-end continuous pharmaceutical pilot plant. The ratio is automatically determined and implemented based on a concentration control loop with a UV flow cell as a key PAT tool. Each point represents the median value of a series of data points collected within 100 min with a sampling frequency of 0.1 Hz. The PI-control loop uses a gain of 51 g/g and an integration time of 60 s.

the interval, larger jumps with steady periods can be seen. To understand the source of these fluctuations, details about the PAT tools and control loops upstream are required. The settling tank upstream has two level sensors—one level sensor is based on ultrasound and one is a floating bulb level sensor. The latter sensor has limited resolution in our application and combined with the high gain of the controller results in the sudden jumps in the flow rate of solvent. The jumps in the second part of the plotted time interval correspond to discrete changes in the aqueous level which cause the flow rate of the aqueous phase out of the settling tank to change suddenly. Consequently, the flow rate of C1 solution will change as well to maintain the total level in the settling tank at a desired set point. Finally, short interruptions are caused by manual interventions in the process (e.g., at 49.7 h) related to cleaning of the microfiltration membrane modules. The fluctuations in the flow rate ratio are smaller (Figure 4C). A general downward trend can be observed, which is mainly caused by the set point changes (Figure 4A).

In summary, our experimental findings demonstrate that the combined feedforward and feedback cascade control loop is effective in maintaining this CMA (i.e., concentration of C1) close to a desired set point, which is done in the presence of both fast and slow disturbances from upstream units and set point changes during a sustained period of operation.

Feedforward Control for Dosage of Fumaric Acid. The reactive crystallization of C3 incorporates two steps—reactive formation of the C3 and the subsequent crystallization of the salt. In our process, the salt formation reaction and the crystallization of the final drug substance occur simultaneously in Crystallizer 3. On the basis of the reaction stoichiometry (Figure 1), the aliskiren free base and fumaric acid (C1 and C2) feed streams should be dosed in a molar ratio of 0.5:1 of C2/C1 to form the aliskiren hemifumarate (C3). The ratio C2/C1 was set to 0.55:1 to ensure the salt formation reaction is completed.

Experimental results (Figure 5) indicate that the molar ratio C2/C1 has a strong influence on the C3 salt formation and process yield. For a molar ratio C2/C1 less than 0.5, there is not enough fumaric acid to form the C3 hemifumarate salt causing the process yield to decrease. However, if the molar ratio C2/C1 is higher than 0.5, the formation of fumarate, instead of hemifumarate, results in less C3 formed and crystallized.

In batch processes, accurate control of stoichiometry is simpler, as the composition can be adjusted after addition. Continuous processes require additional control to ensure stoichiometry is maintained at all times. In a fully integrated continuous process, the variation of C1 concentration or variation of flow rate from upstream units can easily disrupt the C2/C1 ratio. Therefore, tight control of the C2 dosage is required to reject disturbances in flow and concentration coming from upstream units.

dx.doi.org/10.1021/cg401571h | Cryst. Growth Des. 2014, 14, 2148−2157

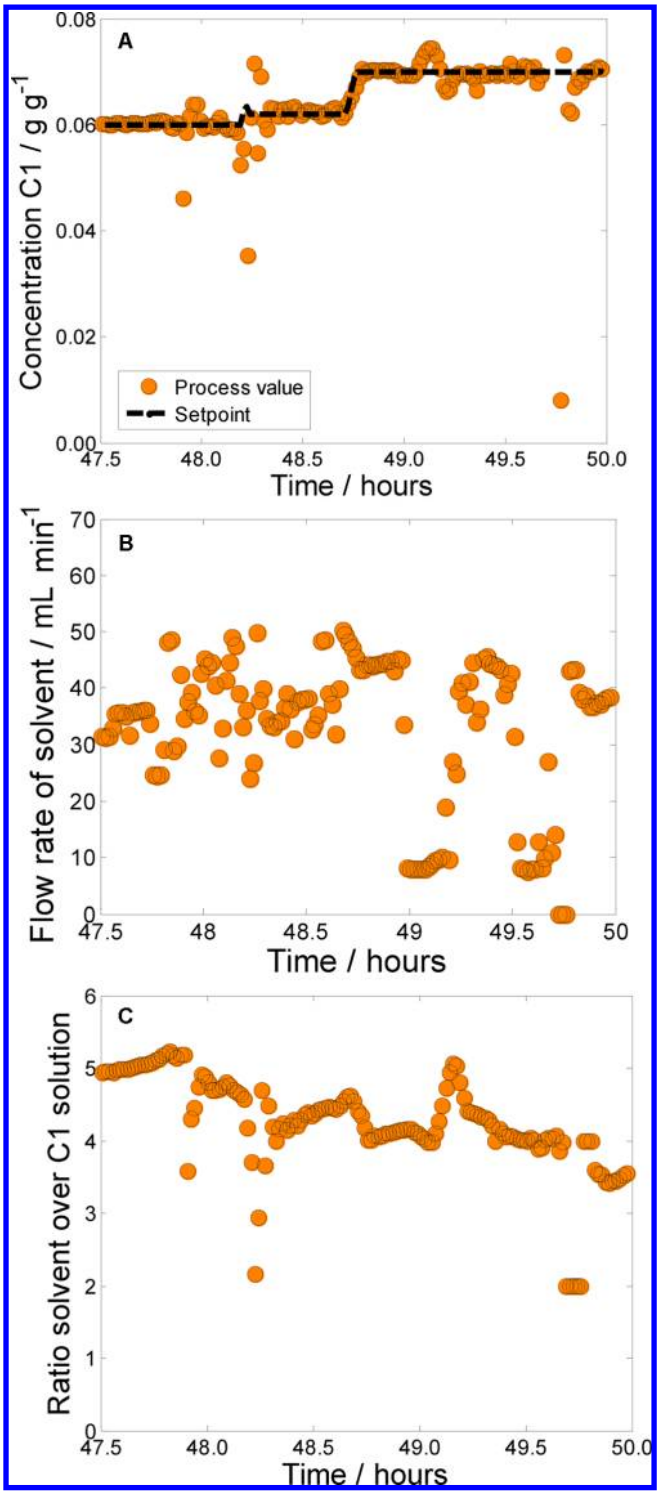

Figure 4. (A) C1 concentration (controlled variable) before entering the dehydration column in a selected time interval during an integrated run of the end-to-end continuous pharmaceutical pilot plant. Two set point changes were implemented during the plotted interval. Each point represents the median value of a series of data points collected within 1 min with a sampling frequency of 0.1 Hz. The PI-control loop uses a gain of 51 g/g and an integration time of 60 s. (B) Flow rate of solvent (manipulated variable) added to dilute the solution of C1 going into the dehydration column in a selected time interval during an integrated run of the end-to-end continuous pharmaceutical pilot plant. Each point represents the median value of a series of data points collected within 1 min with a sampling frequency of 0.1 Hz. (C) Ratio of the flow rate of a solvent feed stream over the flow rate of C1 solution (manipulated variable) coming from upstream units in a selected time interval during an integrated run of the end-to-end continuous pharmaceutical pilot plant. The ratio is automatically determined and implemented based on a concentration control loop with a UV flow cell as key PAT tool. Each point represents the median value of a series of data points collected within 1 min with a sampling frequency of 0.1 Hz. The PI-control loop uses a gain of 51 g/g and an integration time of 60 s.

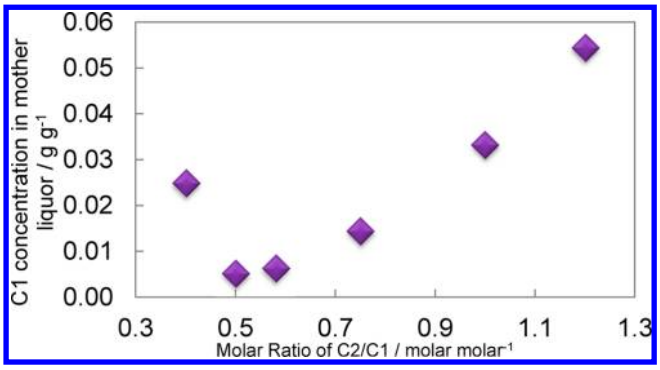

Figure 5. Influence of molar ratio of C2/C1 on C3 salt formation at 20 °C.

Figure 6 presents the flow rate of C1 solution out of the break tank as automatically adjusted via a feedback level control

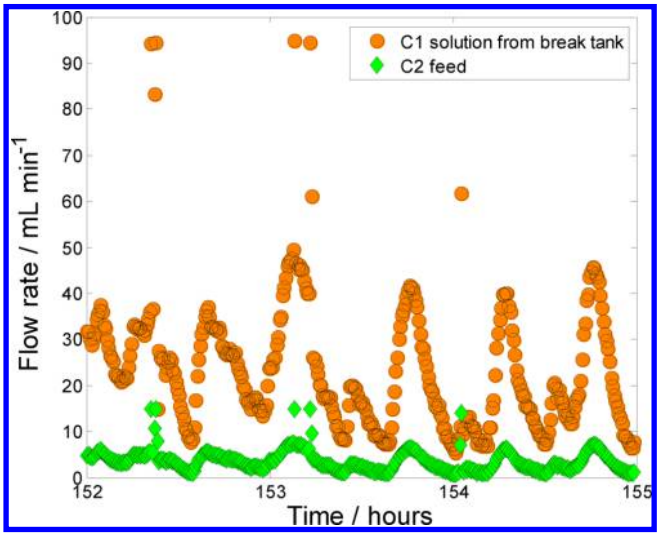

Figure 6. Flow rate of C2 solution added to the crystallizers as determined by a feedforward control loop based on the flow rate and concentration of C1 solution from the break tank. Each point represents the median value of a series of data points collected within 30 s with a sampling frequency of 0.1 Hz. The proportional control loop that controls the level of the break tank uses a gain of 0.0033 s^{-1}.

loop and the flow rate of C2 solution as determined by eq 1 for a selected time interval where large dynamics in these flow rates were observed. The flow rate of C1 solution out of the break tank fluctuates significantly, which is believed to be caused by the level controllers of the settling tank upstream as explained in the previous section and possibly by surging of the dehydration column. The purpose of surging the column is to release the gas in the column, which causes the fluctuation of the C1 solution flow rate. The obvious outlier points are due to

dx.doi.org/10.1021/cg401571h | Cryst. Growth Des. 2014, 14, 2148−2157

temporary misreading of the level by the ultrasonic level sensors. Figure 7 shows the changes in C1 concentration of the

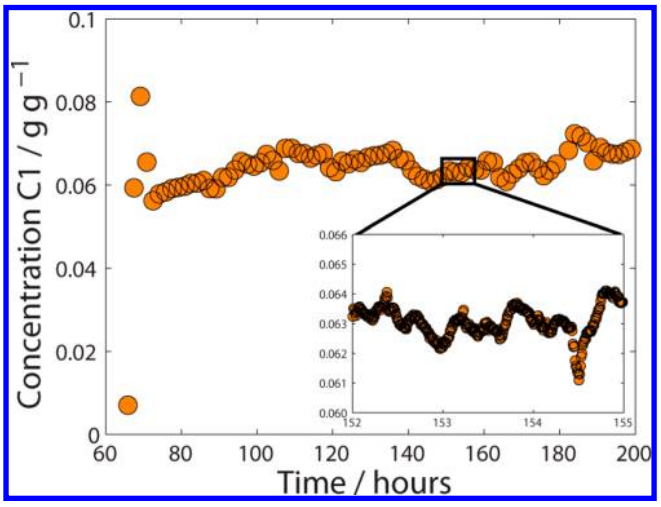

Figure 7. Concentration of C1 in the solution leaving the break tank over 140 h of operation during an integrated run of the end-to-end ICM pilot plant. Each point represents the median value of a series of data points collected within 100 min with a sampling frequency of 0.1 Hz. The inset shows the concentration for a selected time interval where each point represents the median value of a series of data points collected within 30 s.

stream that leaves the break tank as measured by the UV flow cell. The fluctuations in concentration are much smaller than the fluctuations in flow rate both in the selected time interval and in the long term performance. Consequently, the fluctuations in the flow rate of C2 solution going into Crystallizer 3 are mainly the result of the fluctuating flow rate of C1 solution out of the break tank. The combination of fast fluctuations in flow rates and slow fluctuations in concentration demonstrates the importance of automated feedforward control that takes into account both flow rate and concentration of C1 to dose C2 for the reactive-crystallization step.

In Figure 8, the real-time yield in the crystallization process during the run is presented. The yield is tightly related to the ratio C2/C1. Deviations in the ratio lead to a dramatic decrease in the process yield. However, with tight control over the C2 addition, the continuous crystallization process yield reaches 91.4% at the pilot plant scale in this particular run, which is

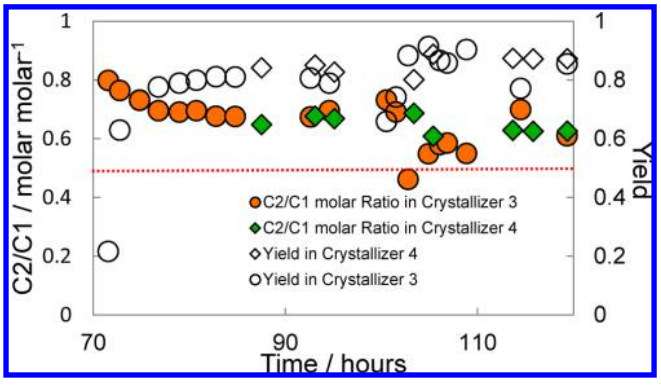

Figure 8. Influence of the C2/C1 molar ratio on the yield in the two stages of crystallization. Note: the dashed red line is the target C2/C1 molar ratio level.

consistent with the results measured at bench scale. We have achieved a yield as high as 92.3% in the bench-scale experiments, which is predicted by the process modeling results.[8]

Level Control in the Two-Stage MSMPR Crystallization System. To guarantee long-term stable operation of the continuous crystallizers, level control has to be implemented. The set points for the level controllers determine the residence times of the crystallizers, which are important parameters affecting crystallization performance such as crystal size distribution and yield. In addition, a large residence time in the crystallizers can act as a buffer to absorb large fluctuations in flow rate. Figure 9A illustrates the measured level of both crystallizers during a period in which both level control loops were closed and in which strong fluctuations in throughput

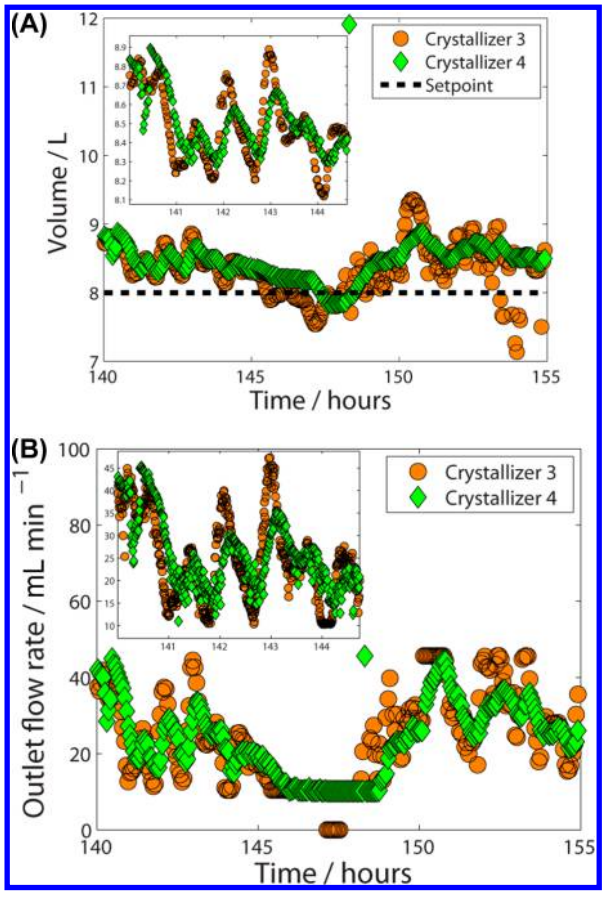

Figure 9. (A) Dynamic development of the measured level in Crystallizers 3 and 4 including the desired set point within a selected time interval during an integrated run of an end-to-end continuous pharmaceutical pilot plant. Each point represents the median value of a series of data points collected within 200 s with a sampling frequency of 0.1 Hz. The inset presents the initial behavior in more detail (median taken out of 30 s of data collection). The P-control loops on the level of the crystallizers use a gain of 0.00083 s^{-1}. (B) Dynamic development of the outlet flow rate of Crystallizers 3 and 4 (manipulated variables of level control loops) within a selected time interval during an integrated run of an end-to-end continuous pharmaceutical pilot plant. Each point represents the median value of a series of data points collected within 200 s with a sampling frequency of 0.1 Hz. The inset presents the initial behavior in more detail (median taken out of 30 s of data collection). The P-control loops that control the level of the crystallizers use a gain of 0.00083 s^{-1}.

dx.doi.org/10.1021/cg401571h | *Cryst. Growth Des.* 2014, 14, 2148−2157

from upstream units are observed. Proportional-only control is applied, which results in a steady-state offset between the manipulated variable and the set point. In the first hours of the plotted time interval, oscillations in the level of both crystallizers have a frequency in the same order of magnitude as the flow rate out of the break tank (Figure 6). The level of both crystallizers oscillate with the same frequency, and the amplitude of the oscillations is typically the largest in Crystallizer 3 (see inset of Figure 9A). The dampening of the oscillations is the result of the buffering capacity of the crystallizers in combination with a small gain in the feedback level control loop, which reduces the magnitude of the oscillations leaving the continuous crystallization system. Figure 9B presents the flow rates out of both crystallizers, which are simply proportional to the difference between the measured level and the set point of the level control loop. The fluctuations in flow rate decrease when exiting the continuous crystallization system (see inset of Figure 9B). In the middle of the plotted time interval in Figure 9A,B, a significant disruption reduced the flow rate of C1 solution toward the continuous crystallization system. This resulted in the level dropping below the set point and caused the level controller to saturate at the minimum throughput required for the downstream filtration operation. In the final part of the time interval, a similar behavior as in the beginning was observed.

In summary, feedback level control on each stage of the continuous crystallization system maintains the level within each stage around a desired set point in the presence of significant disturbances in flow rate from upstream units. Each stage acts as a buffer to absorb fluctuations in flow rate.

Control of Solid Loading in Produced API Slurry. After crystallization, the C3 slurry is purified in the combined filtration-wash stage (>99.0 area %, HPLC) and concentrated in a buffer vessel. The weight fraction of C3 in the slurry is a CMA to meet the specifications of the dryer downstream, which motivated the use of an automated control loop involving an online density flow cell to ensure a constant solid loading. A calibration curve for C3 concentration, which has been created with temperature and density, is given by

$$C = \alpha T + \beta\rho + \gamma \quad (2)$$

where C is the concentration of C3, T is the temperature of the solution, ρ is the density, and α, β, and γ are fitted parameters. Figure 10A,B shows the development of the concentration obtained from the online density measurement (controlled variable) and flow rate of solvent (manipulated variable) respectively for a selected time interval including a set point change. The automated control loop is able to maintain the concentration of C3 close to the desired set point. The transient period between the two points of operation lasts for several hours. During that period, the system operates in open-loop mode (Figure 10B) as the system does not have an active mechanism to increase the concentration other than allowing material with a higher concentration to enter the tank from the filter. Nevertheless, the absence of solvent addition is sufficient to drive the concentration up to the new desired set point.

Product Characterization. The crystals produced in the current pilot-plant continuous crystallization process have been characterized by XRD, optical microscopy, FBRM, and HPLC. The XRD pattern and the microscopic image indicate that the product has a needle-like morphology and a crystalline structure.

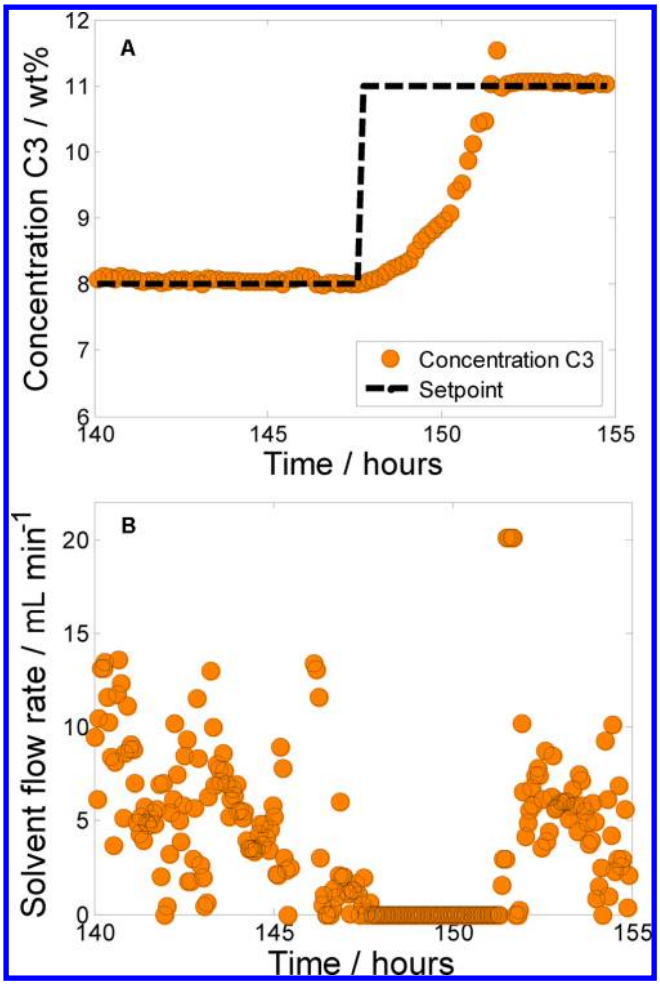

Figure 10. (A) Dynamic development of the C3 concentration in the buffer tank after the continuous crystallization stages for a selected time interval during an integrated run of an end-to-end continuous pharmaceutical pilot plant. Concentration is obtained from an online density measurement (controlled variable). The dashed line represents the set point of the automated feedback control loop. Each point represents the median value of a series of data points collected within 10 min with a sampling frequency of 0.1 Hz. The concentration P-control loop of the buffer tank uses a gain of 0.00017 m^3/s. (B) Dynamic development of the flow rate of solvent to the buffer tank after the continuous crystallization stages (manipulated variable in automated concentration control loop) for a selected time interval during an integrated run of an end-to-end continuous pharmaceutical pilot plant. Each point represents the median value of a series of data points collected within 200 s with a sampling frequency of 0.1 Hz. The P-control loop for the concentration of the buffer tank uses a gain of 0.00017 m^3/s.

Offline FBRM was employed to track the evolution of the particle size distribution by taking samples periodically. It is difficult to implement online FBRM measurements in this case due to the nature of the material. The crystalline product is sticky and easily covered the probe window, which restricted inline measurements. The results from the measurement can be used to assess the performance of the crystallization step and possibly adjust the operational parameters to target a specific size distribution. On the basis of the crystallization kinetics study,[8] we can adjust the operational parameters, such as the residence time, temperature, etc. to control the crystal size distribution, despite aliskiren hemifumarate being a slowly growing crystal. The evolution of the chord length distribution

dx.doi.org/10.1021/cg401571h | Cryst. Growth Des. 2014, 14, 2148−2157

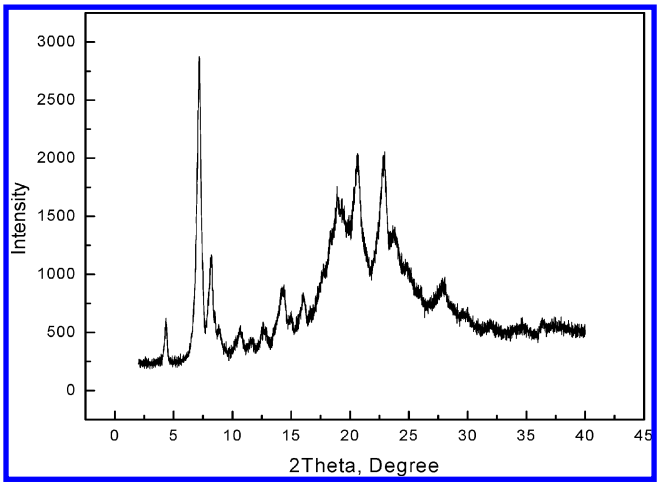

Figure 11. XRD pattern of the final C3 crystals.

presented in Figure 12 indicates that the continuous crystallization process took about 4−5 residence times to

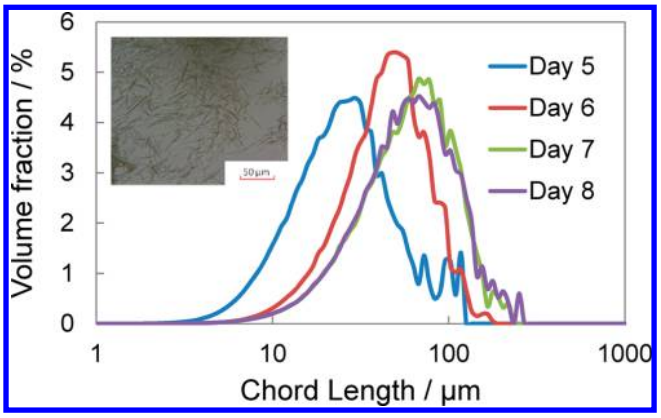

Figure 12. Chord length distribution and microscope image of the final C3 crystals over time.

reach steady-state operation. The crystal size distribution was quite stable after it reached steady state under the operation conditions chosen.

The C3 crystals after crystallization and filtration were sampled periodically, and the purity was measured by HPLC during the entire campaign including, but not limited to, the period required to reach steady. The purpose of the samples was to track the purity profile of the product to ensure that the process was behaving normally. No automatic control loop was set based on the HPLC purity level from the offline measurement. As shown in Figure 13, the purity of the C3 crystals after crystallization and filtration exceeded 99% for most of the tested periods. The low purity after 105 and 125 h was due to the poor performance of the filtration device at those points, which was caused by temporary clogging of its vacuum line.

CONCLUSIONS

A two-stage continuous crystallization system has been successfully integrated in an end-to-end continuous pharmaceutical pilot plant. The API (aliskiren hemifumarate) slurry is required to meet specifications in terms of solid loading, identity, and purity. Furthermore, significant disturbances originating from upstream units that act on the crystallization

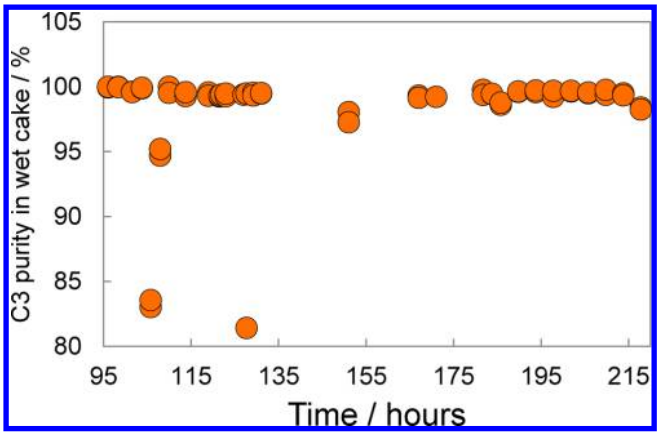

Figure 13. Purity evolution of the C3 wet cake after filtration within a selected time interval during an integrated run of an end-to-end continuous pharmaceutical pilot plant.

section were observed during the integrated run of the pilot plant. Our experimental findings demonstrate that a combined feedforward and feedback automated control loop involving an inline UV measurement controlling the flow rate of a solvent diluent is effective in controlling the concentration of the stream entering the crystallization section in the presence of disturbances. The feedforward control loop mitigates fast disturbances in flow rate, and the feedback control loop mitigated slow disturbances in concentration from upstream units over prolonged periods of operation. Precise dosage of fumaric acid was essential in obtaining a high yield and the desired product identity. A feedforward automated control loop involving a calibrated volumetric pump and an inline UV flow cell allowed for dosage of fumaric acid based on real-time measurements of flow rate and concentration. In particular, the flow rate showed strong fluctuations throughout the run, whereas the concentration obtained from the UV measurement did not fluctuate significantly during the run. Feedback level control loops on each crystallizer absorbed strong fluctuations in inlet flow rate at the expense of fluctuations in the level of both crystallizers. Finally, control of the solid loading of the API slurry after filtration and washing was obtained through a feedback concentration control loop involving an online density measurement using a solvent feed flow rate as the manipulated variable. Steady-state operation in terms of the chord length distribution of the crystals was obtained after about 4−5 residence times, and the process yield achieved 91.4% in this particular run with the purity of the API crystals over 99%.

The continuous reactive-cooling crystallization process of aliskiren hemifumarate with real-time control through PAT tools can effectively maintain steady-state operation. The process produces acceptable C3 crystals with consistent properties. The application of the continuous crystallization in the ICM process of aliskiren hemifumarate has offered great advantages in terms of the manufacturing efficiency, product stability, and process control.

AUTHOR INFORMATION

Corresponding Author

*Present address: #4102 2424 9th Avenue, Longmont, CO 80503, USA. E-mail: James.Evans@hospira.com.

Notes

The authors declare no competing financial interest.

■ ACKNOWLEDGMENTS

We would like to acknowledge Novartis International AG for its generous funding of this research as well as for supplying starting materials. We acknowledge the support of the members of the pilot plant team who contributed to building and operating the plant, namely, Salvatore Mascia, Erin Bell, Megan A. Foley, Ellen Cappo, Corinne Carland, Joshua Dittrich, Ryan Hartman, Devin Hershey, Bowen Huo, Anjani Jha, Ashley S. King, Tushar Kulkarni, Timur Kurzej, Aaron Lamoureux, Paul S. Madenjian, Sean Ogden, Ketan Pimparkar, Joel Putnam, Anna Santiso, Jose C. Sepulveda, Daniel Tam, Kristen Talbot, Justin Quon, and Forrest Whitcher (from MIT). We also thank Dr. Holger Schank for assistance with the HPLC analysis.

■ REFERENCES

(1) Myerson, A. S. Handbook of Industrial Crystallization, 2nd ed.; Butterworth-Heinemann: Boston, 2002.
(2) Chen, J.; Sharma, B.; Evans, J. M. B.; Myerson, A. S. *Cryst. Growth Des.* **2011**, *11* (18), 887−895.
(3) Schaber, S. D.; Gerogiorgis, D. I.; Ramachandran, R.; Evans, J. M. B.; Barton, P. I.; Trout, B. L. *Ind. Eng. Chem. Res.* **2011**, *50* (17), 10083−10092.
(4) Benyahia, B.; Lakerveld, R.; Barton, P. *Ind. Eng. Chem. Res.* **2012**, *51* (47), 15393−15412.
(5) Mascia, S.; Heider, P.; Zhang, H.; Lakerveld, R.; Benyahia, B.; Barton, P.; Braatz, R.; Cooney, C.; Evans, J.; Jamison, T.; Jensen, K.; Myerson, A.; Trout, B. *Angew. Chem., Int. Ed.* **2013**, *52* (47), 12359−12363.
(6) Alvarez, A. J.; Singh, A.; Myerson, A. S. *Cryst. Growth Des.* **2011**, *11* (10), 4392−4400.
(7) Zhang, H.; Quon, J.; Alvarez, A. J.; Evans, J.; Myerson, A. S.; Trout, B. *Org. Process Res. Dev.* **2012**, *16*, 915−924.
(8) Quon, J. L.; Zhang, H.; Alvarez, A.; Evans, J.; Myerson, A.; Trout, B. L. *Cryst. Growth Des.* **2012**, *12*, 3036−3044.
(9) Wong, S. Y.; Tatusko, A. P.; Trout, B. L.; Myerson, A. S. *Cryst. Growth Des.* **2012**, *12* (11), 5701−5707.
(10) Alvarez, A. J.; Myerson, A. S. *Cryst. Growth Des.* **2010**, *10* (5), 2219−2228.
(11) Lawton, S.; Steele, G.; Shering, P.; Zhao, L. H.; Laird, I.; Ni, X. W. *Org. Process Res. Dev.* **2009**, *13*, 1357−1363.
(12) Tavare, N. S. *AIChE J.* **1986**, *32*, 705−732.
(13) Sheikh, A. Y.; Jones, A. G. *AIChE J.* **1998**, *44*, 1637−1645.
(14) Kougoulos, E.; Jones, A. G.; Wood-Kaczmar, M. W. *Org. Process Res. Dev.* **2006**, *10* (4), 739−750.
(15) Ward, J. D.; Yu, C. C.; Doherty, M. F. *AIChE J.* **2007**, *53* (11), 2885−2896.
(16) Samad, N. A. F. A.; Sin, G.; Gernaey, K. V.; Gani, R. *Comput. Chem. Eng.* **2013**, *54*, 8−23.
(17) Johnson, M. D.; May, S. A.; Calvin, J. R.; Remacle, J.; Stout, J. R.; Diseroad, W. D.; Zaborenko, N.; Haeberle, B. D.; Sun, W. M.; Miller, M. T.; Brennan, J. *Org. Process Res. Dev.* **2012**, *16* (5), 1017−1038.
(18) Variankaval, N.; Cote, A.; Doherty, M. F. *AIChE J.* **2008**, *54* (7), 1682−1688.
(19) Nagy, Z. K.; Braatz, R. D. *Annu. Rev. Chem. Biomol. Eng.* **2012**, *3*, 55−75.
(20) Braatz, R. D. *Annu. Rev. Control* **2002**, *26*, 87−99.
(21) Hojjati, H.; Sheikhzadeh, M.; Rohani, S. *Ind. Eng. Chem. Res.* **2007**, *46* (4), 1232−1240.
(22) Rohani, S.; Horne, S.; Murthy, K. *Org. Process Res. Dev.* **2005**, *9*, 858−872.
(23) Doki, N.; Seki, H.; Takano, K.; Asatani, H.; Yokota, M.; Kubota, N. *Cryst. Growth Des.* **2004**, *4* (5), 949−953.
(24) Cimarosti, Z.; Rossi, S.; Tramarin, D.; Laval, G.; Stabile, P.; Giubellina, N.; Maton, W.; Allieri, B.; Campi, F.; Cooke, J.; Westerduin, P. *Org. Process Res. Dev.* **2012**, *16* (10), 1598−1606.
(25) Helmdach, L.; Feth, M. P.; Ulrich, J. *Org. Process Res. Dev.* **2013**, *17* (3), 585−598.
(26) Lin, S. W.; Ng, K. M.; Wibowo, C. *Ind. Eng. Chem. Res.* **2007**, *46* (2), 518−529.
(27) Lakerveld, R.; Benyahia, B.; Braatz, R. D.; Barton, P. I. *AIChE J.* **2013**, *59* (10), 3671−3685.
(28) Heider, P.; Born, S.; Basak, S.; Benyahia, B.; Lakerveld, R.; Zhang, H.; Hogan, R.; Buchbinder, L.; Wolfe, A.; Evans, J.; Jamison, T.; Jensen, K. *Org. Process Res. Dev.* **2014**, *18*, 402−409.
(29) Couper, J. R.; Penney, W. R.; Fair, J. R.; Walas, S. M. *Chemical Process Equipment: Selection and Design*, 2nd ed.; Elsevier: Burlington, MA, 2005.
(30) Zwietering, Th. N. Suspending of solid particles in liquid by agitators. *Chem. Eng. Sci.* **1958**, *9* (3−4), 244−253.
(31) Paul, E. L.; Atiemo-Obeng, V. A.; Kresta, S. M. Handbook of Industrial Mixing. In *Science and Practice*; John Wiley & Sons Inc: Hoboken, NJ. 2003.
(32) Togkalidou, T.; Tung, H.-H.; Sun, Y.; Andrews, A.; Braatz, R. D. *Ind. Eng. Chem. Res.* **2004**, *43*, 6168−6181.
(33) Kempkes, M.; Eggers, J.; Mazzotti, M. *Chem. Eng. Sci.* **2008**, *63*, 4656−4675.
(34) Barrett, P.; Glennon, B. *Part. Part. Syst. Charact.* **1999**, *16*, 207−211.
(35) Liu, W.; Clark, N. N.; Karamavruc, A. I. *Chem. Eng. Sci.* **1998**, *53*, 1267−1276.
(36) Hukkanen, E. J.; Braatz, R. D. *Sensors Actuators B* **2003**, *96*, 451−459.